Relation of nNOS isoforms to mitochondrial density and PGC-1alpha expression in striated muscles of mice

Oliver Baum[1*], Dea Aaldijk[2¶], Anna Lena Engeli[2¶], Matthias Spree[1], Serge Summermatter[3], Christoph Handschin[3] and Andreas Zakrzewicz[1]

[1] Institute of Physiology
Charité - Universitätsmedizin Berlin
Charitéplatz 1
D-10117 Berlin
Germany

[2] Institute of Anatomy
University of Bern
Baltzerstrasse 2
CH-3009 Bern
Switzerland

[3] Division of Pharmacology/Neurobiology
Biozentrum
University of Basel
Klingelbergstrasse 50/70
CH-4056 Basel
Switzerland

[¶] Dea Aaldijk and Anna Lena Engeli contributed equally to this paper

*** Corresponding author:**
Dr. Oliver Baum
oliver.baum@charite.de

Abstract

The expression of neuronal NO synthase (nNOS) alpha- and beta-isoforms in skeletal muscle is well documented but only little information is available about their regulation/functions. Using different mouse models, we now assessed whether the expression of nNOS-isoforms in muscle fibers is related to mitochondria content/activity and regulated by peroxisome proliferator-activated receptor gamma coactivator-1alpha (PGC-1alpha). Catalytic histochemistry revealed highest nNOS-concentrations to be present in type-2 oxidative muscle fibers. Differences in mitochondrial density between nNOS-KO-mice and WT-littermates established by morphometry after transmission electron microscopy were significant in the oxidative portion of the tibialis anterior muscle (TA) but not in rectus femoris muscle (RF) indicating an nNOS-dependent mitochondrial pool in TA. Quantitative immunoblotting displayed the nNOS alpha-isoform to preponderate in those striated muscles of C57Bl/6-mice that comprise of many type-2 oxidative fibers, e.g. TA, while roughly even levels of the two nNOS-isoforms were expressed in those muscles that mainly consist of type-2 glycolytic fibers, e.g. RF. Differences in citrate synthase-activity in muscle homogenates between nNOS-KO-mice and WT-littermates were positively related to nNOS alpha-isoform levels. In transgenic-mice over-expressing muscular PGC-1alpha compared to WT-littermates, immunoblotting revealed a significant shift in nNOS-expression in favor of the alpha-isoform in six out of eight striated muscles (exceptions: soleus muscle and tongue) without consistent relationship to changes in the expression of mitochondrial markers. In summary, our study demonstrated the nNOS alpha-isoform expression to be related to mitochondrial content/activity and to be up-regulated by up-stream PGC-1alpha in striated muscles, particularly in those enriched with type-2 oxidative fibers implying a functional convergence of the two signaling systems in these fibers.

Key words

neuronal nitric oxide synthase (nNOS)

nNOS alpha- and beta-isoforms

skeletal muscle

mitochondria

peroxisome proliferator-activated receptor gamma coactivator-1alpha (PGC-1alpha)

Abbreviations

NO, nitric oxide; nNOS, neuronal nitric oxide synthase; PGC-1alpha, peroxisome proliferator-activated receptor gamma coactivator-1alpha; KO, knockout; TG, transgenic; CS, citrate synthase; SDH, succinate dehydrogenase; ROS, reactive oxygen species; NBT, nitroblue tetrazolium; TEM, transmission electron microscopy; TA, tibialis anterior muscle; RF, rectus femoris muscle; EDL, extensor digitorum longus muscle; PLNT, plantaris muscle; SOL, soleus muscle; GC, gastrocnemius muscle

Highlights

- Highest nNOS-levels are expressed in type-2 oxidative fibers in striated muscles of mice
- Muscle nNOS-alpha isoform is positively related to differences in citrate synthase-activity between nNOS-KO-mice and WT-littermates
- nNOS alpha-isoform preponderates in striated muscles with many type-2 oxidative fibers
- In muscles of PGC-1alpha transgenic mice, nNOS-expression is shifted in favor of the alpha-isoform without consistent relationship to changes in the expression of mitochondrial markers

1. Introduction

Gaseous nitric oxide (NO) is generated by the catalytic activity of neuronal NO synthase (nNOS) in skeletal muscles of rodents and humans. Dimer aggregates of nNOS are clustered at the sarcolemma, especially in fast-twitch (type-2) oxidative muscle fibers of rodents [1; 2]. The fiber surface targeting of nNOS is mediated either indirectly via interaction with alpha-syntrophin [3] and/or other adapter proteins [4] or by direct binding to dystrophin [5; 6; 7] and is pivotal for its correct and integrated function. Accordingly, variations in the sarcolemmal anchorage of nNOS contribute to the etiology and progression of several distinctive muscular dystrophies [8; 9; 10].

As a pleiotropic second messenger, NO produced by nNOS-activity influences via the established soluble guanylate cyclase/cGMP-signaling cascade [11] and/or S-nitrosylation of enzymes and fibrillar proteins in skeletal muscle fibers [12]. As a result, several reactions of the oxidative metabolism in skeletal muscle fibers are modulated at different levels, e.g. to establish an intact mitochondrial phenotype [13; 14], although the integration of nNOS action into the cell signaling network that controls the oxidative phenotype of muscle fibers is currently only partially understood [15]. Because nNOS exerts also a positive effect on sarcomeric assembly in vitro [16], it has been speculated that the nNOS/NO system influences hypertrophy [17] and age-related sarcopenia [18]. Other studies revealed that nNOS-generated NO also acts as a paracrine signaling molecule that impacts the microvascular system in skeletal muscle [19; 20]. Taken together, nNOS may influence simultaneously the phenotype and function of both the muscle fibers and the microcirculation in skeletal muscle at several levels and is thus an enzyme that is well positioned to modulate the interplay between the two tissues. This integrative character of the nNOS/NO-system in skeletal muscle is especially relevant for the higher requirement of oxygen and substrates during endurance exercise [21].

Studies using nNOS-KO mice [22] and nNOS-overexpressing transgenic mice [23] have previously shown that an alteration of nNOS expression levels in skeletal muscle is accompanied by a change in the availability of superoxide and, subsequently, hydrogen peroxide (SOD-1 dependent) and/or peroxynitrite. Thus, nNOS participates in the scavenging of reactive oxygen species (ROS), which could damage proteins and lipids within the skeletal muscle fibers [24]. Because ROS also exert important cell signaling functions, the nNOS/NO system may act not only as

direct but also indirect (by depletion of ROS) modulator of cell signaling processes [25].

Various isoforms of nNOS are expressed in skeletal muscle. Among the nine nNOS-variants with the alternatively spliced non-translated exon-1 being present in humans [26], only four (1b, 1c, 1g and 1h) mRNA-variants were likewise found in the mouse [3]. At the protein level, two major nNOS-isoforms have been identified in human and mouse striated muscles: alpha (160 kDa) and beta-isoforms (140 kDa) of nNOS that differ in the presence/absence of a 237 amino acid long stretch at the N-terminus which is generated by alternative splicing of exon-2 [3]. Both alpha- and beta-variants of nNOS might display a 102-bp long nucleotide stretch (designated exon-mu) subjected to alternative splicing between exons 16 and 17 [27].

The additional exon-2 of the nNOS alpha-isoform contains a PDZ domain that mediates the fiber surface targeting [3]. The physiology of the nNOS alpha-isoform is well studied [15]: due to its sarcolemmal anchorage this enzyme or rather its reaction product NO impacts the metabolic demands of the striated musculature, as mentioned above. In contrast, the beta-variant of nNOS has not been thoroughly characterized so far - a circumstance that reflects the non-availability of a specific antibody against this nNOS-isoform.

There is only few and partly conflicting information available about distinctive expression patterns, biochemical properties and functional relevance in skeletal muscle of these nNOS-variants. Recombinant alpha and beta-isoforms of nNOS exhibit NOS activity with similar catalytic properties in homogenates of transfected COS-cells [3]. Percival et al. have attributed a Golgi apparatus-associated localization in muscle fibers of the nNOS beta-isoform and a role in force maintenance during and after exercise in mice [28]. However, this interpretation of the data of this is largely speculative, since no information regarding the expression of the beta-isoform was furnished at either the mRNA or protein level. Using a set of antibodies that recognize either only the alpha-isoform or simultaneously both nNOS-variants, we have found evidence that both nNOS-isoforms are associated at the sarcolemma [29] possibly acting as a heterodimer. The reason for the differences in the determination of nNOS isoform localization in skeletal muscle fibers [28; 29] remains to be clarified.

The incomplete characterization of the nNOS action within the oxidative metabolism as well as the fragmented knowledge about the biochemistry of the nNOS-variants in

skeletal muscles provided so far has encouraged us to speculate that the appearance of one or both nNOS-isoforms is/are related to the mitochondrial phenotype of this tissue. To address this hypothesis, we first systematically monitored the expression patterns of the two major isoforms in several striated muscles of mice with different metabolic profiles to relate these data to the mitochondrial density in these tissues. In order to obtain insights into the regulation of the nNOS isoform-specific expression patterns, we have also characterized the interaction of the alpha- and beta-isoforms of nNOS with PGC-1alpha, a master regulator gene of mitochondrial biogenesis [30; 31]. Our analysis reveals that the expression of the nNOS alpha-isoform is positively related to mitochondria density and PGC-1alpha expression in striated muscles with many type-2 fibers, suggesting a close connection between the nNOS alpha-isoform and the oxidative capacity in type-2-rich skeletal muscles, which has hitherto not been described.

2. Materials and methods

2.1 Animals

Histochemical, electron microscopy and biochemical studies were performed on striated muscles from male C57/BL6 mice in the age of nine weeks (Charles River, Sulzfeld, Germany).

The nNOS-knockout (KO) strain of mice with C57BL/6-background utilized in this study was originally generated by the recombinant replacement of exon-2 of the nNOS-gene with a neomycin cassette [32]. We purchased a founder generation of these mice from Jackson Laboratories, Bar Harbor, ME, USA. By inbreeding of heterozygous (C57BL/6-WT x nNOS-KO) mice (F1-offsprings), seven litters were obtained (F2-offsprings) which were subjected to genotyping using DNA from biopsies of the tail tips **(Supplementary Fig. 1)**. The homozygous male mice of these litters were euthanized at the age of 16-weeks to collect the skeletal muscles for molecular and structural analyses [33].

The keeping of the muscle-specific PGC-1alpha (PGC-1alpha) transgenic (TG) mice and their WT littermates was previously described [34].

All mice were maintained in conventional animal facilities in Bern or Zurich, respectively, with a fixed 12-h light/dark cycle on a commercial pelleted chow diet with free access to tap water. At sacrifice, mice were anesthetized with a ketamine/xylazine (100 mg*kg-1/5 mg*kg-1) cocktail via IP injection. All mice were treated and sacrificed in accordance with the approvals published by the Cantonal Committee on Animal Welfare [Amt für Landwirtschaft und Natur des Kantons Bern (51/08 and 27/12)] and the Universities of Bern and Zurich.

2.2 Muscles

For the analyses, the following striated muscles of the nNOS-KO mice and their WT littermates as well as PGC-1alpha-TG mice and their WT littermates were used: tibialis anterior (TA), extensor digitorum longus (EDL), rectus femoris (RF) of the quadriceps femoris, plantaris (PLNT), soleus (SOL), gastrocnemius (GC) - caput lateralis (lat) and caput medialis (med) and the tongue.

2.3 Histochemistry

For succinate dehydrogenase (SDH) histochemistry, unfixed cryostat sections of 10 µm thickness were incubated in a moist chamber with SDH medium (1.5 mg/ml

sodium-succinate, 0.25 mg/ml nitroblue tetrazolium (NBT) salt in 0.1 M phosphate buffer, pH 7.2) at 37°C for 30 min, then washed with deionized water and finally cover-slipped in glycerol gelatin.

NADPH diaphorase histochemistry specific for nNOS was carried out using 1 M urea in the incubation buffer as previously reported [35]. Quantification of SDH and nNOS-diaphorase histochemical activity in individual muscle fibers was performed by image analysis as previously described in detail [2].

2.4 Electron microscopy and morphometry

TA and RF muscles were subjected to transmission electron microscopy (TEM) analysis. Therefore, TA muscle was longitudinally sliced to obtain the oxidative proportion (originally adjacent to the tibia), which was processed for TEM analysis. Ultrathin sections (50-60 nm in thickness) of Epon resin blocks of the muscles were prepared as previously described [36]. The inspection of the Epon blocks was carried out using a transmission electron microscope (Morgagni M268; FEI, Brno, Czech Republic). Morphometric estimation of the mean volume density (Vv) of mitochondria on 20 randomly depicted micrographs taken of each of the ultrathin sections, at a magnification of x24,000, were also carried out using established methods as previously described [36].

2.5 Immunoblotting

The muscles were homogenized in solubilization buffer (1% (w/v) Triton-X 100 and 1 mM phenylmethylsulfonyl fluoride in PBS-HCl, pH 7.4), as previously described [33]. Immunoblotting was performed using 50 µg of protein from skeletal muscles. The blot matrices were incubated with the following primary anti-nNOS antibody in final 0.1 µg/ml concentration diluted in washing buffer (0.1% (w/v) Tween 20 in PBS, pH 7.4) overnight at 4°C: N-7280 (Sigma-Aldrich, Buchs, Switzerland), which specifically identifies amino acids 1409-1429 in the C-terminal region of the rat and mouse primary structure or with the mitochondria-specific OXPHOS Rodent WB Antibody Cocktail (ab110413; Abcam, Cambridge, UK), diluted 1:1.000 in washing buffer.

The immunoblots were developed by enhanced chemiluminescence (GE Healthcare Life Sciences, Glattbrugg, Switzerland). Ponceau S-staining of the blot matrices was conducted for the normalization of the loading required for the densitometric quantification [33].

2.6 Citrate synthase activity assay

Approximately 10 mg of the muscles were homogenized in 500 ml of 100 mM Tris-buffered saline, pH 8.3 (TBS) and 0.1% Triton X-100 at 4°C using a Polytron ultraturrax PT 1200 E (Kinematica, Luzern, Switzerland). Subsequently, the lysates were centrifuged at 14.000 rpm for 5 min at 4°C to subject aliquots of the supernatants to the CS activity assay and BCA protein assay. CS activity was determined spectrophotometrically at 30°C by measuring the appearance of mercaptide ion by acetyl-CoA deacylase activity according to the protocol described previously in detail [37].

2.7 Nitrate/nitrite fluorometric assay

The nitrate/nitrite fluorometric assay (780051) from Cayman (Ann Arbor, MI, USA) was used as indirect measure for NO production. Therefore, approximately one third of a RF muscle per mouse was homogenized in 5 ml PBS, pH 7.4 at 4°C. After quantification of the protein concentration in aliquots, NOS activity was initiated by addition of the cofactor mixture to 1 mg of homogenate protein at RT and stopped after 15 min by centrifugation through ultrafiltration tubes (UFC703008, Centricon Plus-70, Merck, Darmstadt, Germany). Aliquots of the supernatants collected at initiation and termination of the reaction as well as nitrate standards were subjected in duplicates to the nitrate/nitrite fluorometric assay according to the instructions of the manufacturer. The extinction of the samples was recorded at an excitation wavelength of 360-365 nm and an emission wavelength of 430 nm in a SpectraMax 190 Microplate Reader (Molecular Devices, Sunnyvale, CA, USA) and used to calculate the rates of nitrate/nitrite production per time unit and mg of homogenate protein.

2.8 Data analysis and statistics

All numerical data were expressed as mean values together with the standard deviation. Parameters pertaining to the structural and molecular analyses were compared using a paired Student's *t*-test. Pearson's correlation was calculated to assess significance of relationship. The significance level was set at $P \leq 0.05$.

3 Results

3.1 Relationship of nNOS and mitochondria in skeletal muscles

For assessment of the nNOS/mitochondria relationship at the muscle fiber level, we performed nNOS-specific diaphorase and succinate dehydrogenase (SDH; mitochondrial marker) catalytic histochemistry on serial sections of the tibialis anterior (TA) muscle, which is a skeletal muscle that is almost exclusively composed of type-2 muscle fibers [38]. As shown in **Fig 1A**, nNOS-specific diaphorase activity was exclusively located at the sarcolemma, whereas SDH activity was present inside the muscle fibers (**Fig 1B)**. In both histochemical reactions, the end product formazan was not uniformly distributed within the muscle: the smaller skeletal muscle fibers contained high nNOS and SDH activities, while the larger ones showed only slight formazan generation. As exemplarily displayed for one TA muscle (**Fig 1D), r**egression analysis with both catalytic histochemistry data sets revealed the expression of nNOS to be significantly ($P \leq 0.05$) related to the SDH-defined oxidative capacity at the muscle fiber level.

To extend the investigation on nNOS/mitochondria relationship to the total muscle level, the ultrastructural phenotypes of two exemplary striated muscles were compared in nNOS-KO mice and WT mice **(Fig 2A).** When the compartmental composition of the skeletal muscle fibers in the oxidative portion of the TA muscle (rich in type-2 oxidative fibers) was assessed by morphometry, significantly less (-9.6%; $P \leq 0.05$) mitochondria volume density was found in nNOS-KO mice than in WT mice **(Fig 2B).** While the intrafibrillar pool of mitochondria was significantly lower (-9.9%; $P \leq 0.05$), the subsarcolemmal pool only tended to be reduced (-5.7%; $P = 0.08$) in the nNOS-KO strain compared to the WT mice. In contrast, the morphometric analysis of the rectus femoris (RF) muscle (rich in glycolytic type-2 fibers) revealed the mitochondrial volume density to only non-significantly differ (+6.1%; $P > 0.05$) between the two mouse strains **(Fig 2C).** These data indicate that the manifestation of the nNOS/NO-system in skeletal muscle of WT mice has a promotional effect on mitochondrial density in oxidative TA muscle but not glycolytic RF muscle.

The expression patterns of nNOS in murine striated muscles were assessed by quantitative immunoblotting on detergent extracts of eight striated muscles (seven skeletal muscles of the hind limb and the tongue) from C57Bl/6-mice. As shown in **Fig 3A**, nNOS was consistently displayed in all muscle extracts as a double band with sizes of 160-kDa (alpha-isoform) and 140-kDa (beta-isoform). Although identical

amounts of protein were loaded on the gels, the intensities of the nNOS-immunoreactive bands varied greatly between the muscles. Actually, densitometric analysis **(Fig 3B)** revealed highest levels of nNOS to be present in TA muscle, whereas moderate-high levels of nNOS (44-72% of concentration in TA) were expressed in RF, extensor digitorum longus (EDL), plantaris (PLNT), gastrocnemius (GC)-lateralis muscles and tongue. Only very low levels of nNOS were displayed in GC-medialis (11% of concentration in TA) and soleus (SOL; 4% of concentration in TA) muscles as anticipated, since both muscles consist to a large extent of nNOS-poor, type-1 muscle fibers.

3.2 Relationship of nNOS-isoforms and mitochondria in skeletal muscles

The ratio of nNOS alpha- and beta-isoform expression in the immunoblots was not constant in the muscle samples. As assessed by densitometry **(Fig 3C)**, nNOS alpha-isoform expression preponderated in most muscles (TA, EDL, GC-lat, GC-med, SOL and tongue; 69 up to 91% versus 31 up to 9%), while roughly equal levels of the two nNOS-isoforms were expressed in RF (41% versus 59%) and PLNT muscles (56% versus 44%).

We furthermore measured the citrate synthase (CS) activity (another mitochondrial marker enzyme) by an *in vitro*-assay in homogenates of eight striated muscles isolated from nNOS-KO mice and their WT littermates **(Fig 4A).** While the differences in CS activity between the two mouse strains were only non-significant ($P>0.05$) in most muscle homogenates (+6% up to -12% in nNOS-KO versus WT), the CS activity was significantly ($P\leq0.05$) lower in TA (-16%) and GC-lat (-19%) muscle homogenates and tended to be lower ($P=0.09$) in the tongue homogenate (-21%) of the nNOS-KO mice compared to the WT mice.

When we performed regression analysis with the data sets of CS activities in muscle homogenates (shown in Fig 4A) and the quantitative nNOS isoform expression in the muscles of the WT mice determined by immunoblotting (shown in Fig 3C and 3D), we found a significant ($r=0.73$; $P\leq0.05$) positive relation between the nNOS alpha-isoform expression levels and the differences in CS activities between WT mice and nNOS-KO mice (**Fig 4B).** Correspondingly, the nNOS beta-isoform expression levels and the differences in CS activities were negatively related ($P\leq0.05$; data not shown). All other regression analyses (particularly those with the absolute CS activities from the WT mice) yielded only non-significant relationships between nNOS expression

and mitochondrial density (*P*>0.05; data not shown) particularly due to inclusion of the SOL and GC-med values, which consist mainly of oxidative type-1 fibers lacking substantial nNOS-expression [1]. These findings indicate that a pool of mitochondria exists in murine skeletal muscles with many type-2 fibers, which is related to the ratio of the nNOS alpha-isoform-to-beta-isoform expression in the muscle.

3.3 Expression levels of nNOS isoforms in muscles of PGC-1alpha-TG mice

The statistical relationship between nNOS alpha-isoform expression and mitochondrial density/activity in type-2 fibers encouraged us to clarify whether PGC-1alpha (established transcriptional co-activator of mitochondriogenesis) influences the nNOS isoform expression patterns. Therefore, we analyzed detergent extracts of striated muscles from transgenic mice over-expressing PGC-1alpha (PGC-1alpha-TG mice) and their WT littermates by means of quantitative immunoblotting with anti-nNOS antibodies. In a preliminary experiment, we found the nitrite production rates in RF muscle homogenates, in which nNOS alpha- and beta-isoforms occur in an approximately balanced relationship, to differ only non-significantly (9%; *P*>0.05) between the two mouse strains suggesting that the up-regulation of PGC-1alpha does not impact the total NOS activity in this muscle **(Fig. 5A).**

When we assessed the nNOS isoform-composition in detergent extracts of eight striated muscles by quantitative immunoblotting**,** we observed a distinctive shift in the expression patterns of the nNOS-isoforms in the PGC-1alpha-TG mice compared to their WT-littermates: in most striated muscles, the concentration of the alpha-isoform was increased, while the levels of the beta-isoform were simultaneously decreased **(Supplementary Figs. 2 and 3)**. This effect was most pronounced in the RF muscle (**Fig 5B).** Densitometry revealed significantly (*P*≤0.05) higher levels of the nNOS alpha-isoform and simultaneously significantly (*P*≤0.05) lower levels of the beta-isoform to be expressed in six muscles from PGC-1alpha TG mice compared to WT mice **(Fig 5C)**. In contrast, the distribution of the nNOS alpha- and beta-isoforms differed only non-significantly (*P*>0.05) between the two mouse strains in the SOL and the tongue. Interestingly, the expression levels of total nNOS were inconsistent in the striated muscles of PGC-1alpha TG mice compared to WT mice (**Fig 5D**): while in RF, GC-med, SOL and tongue similar nNOS expression levels were displayed in the two mouse strains, significantly lower levels of total nNOS were

found in the other five skeletal muscles of PGC-1alpha TG mice (TA, EDL, GC-lat, PLNT, SOL).

In order to assess whether the shift of nNOS-isoform expression in muscle extracts of PGC-1alpha TG mice is actually related to the PGC-1alpha-dependent increase in mitochondrial density, we performed immunoblotting on the detergent extracts of the different striated muscles with the mitochondria-specific OXPHOS antibody cocktail. Densitometric analysis of the blot matrices revealed that the levels of the mitochondrial proteins were higher in six out of the eight striated muscles of the PGC-1alpha TG mice compared to WT mice **(Supplementary Fig. 4 and Fig 6A,B).** The levels of mitochondrial ATP5A, quantified as a representative example (**Fig 6C)**, differed only non-significantly between the two mouse strains in the soleus muscle and in the tongue, which concurrently exhibited a likewise non-significant shift in the expression of the nNOS isoforms. Accordingly, significant up-regulated ATP5A levels in RF, EDL and TA muscles of PGC-1alpha TG mice were accompanied by significant changes in the nNOS alpha/beta-isoform relationship. However, there were also striking deviations from this co-regulated relationship: GC-lat, GC-med and PLNT muscles exhibited non-significant ATP5A increases in combination with significant nNOS isoform-shifts, suggesting that the increases in mitochondrial density are only inconsistently associated with the altered nNOS-isoform expression patterns in striated muscles of PGC-1alpha TG mice.

4 Discussion

This paper addresses the relationship between nNOS isoforms, mitochondrial density/activity as well as PGC1alpha expression in murine striated muscles. Our investigation resulted in four main findings: 1. nNOS was enriched in striated muscles with a high proportion of type-2 oxidative fibers, 2. differences in mitochondrial density/activity between nNOS-KO mice and their WT littermates were more pronounced in type-2 oxidative than in glycolytic striated muscles, 3. the expression levels of the nNOS alpha-isoform in striated muscles were positively related to the differences in citrate synthase (CS) activity between nNOS-KO mice and their WT littermates and 4. the isoform expression pattern of nNOS was shifted in favor of the alpha-isoform and at the expense of the beta-isoform in striated muscles of transgenic mice over-expressing PGC-1alpha.

4.1 Enrichment of nNOS in muscles with a many type-2 oxidative fibers

Our quantitative immunoblot analysis revealed nNOS to be inconsistently distributed in the striated musculature of C57/Bl6-mice. Lowest levels of nNOS were found in muscles with a high proportion of type-1 muscle fibers (e.g. SOL, GC-med [38]), which is in accordance to the observation that only low nNOS concentrations are expressed in this fiber type in murine striated muscles [1]. In contrast, high levels of nNOS expression were confined to skeletal muscles with a high proportion of oxidative type-2 fibers, e.g. to TA muscle which consists of 40% of type-2d/x and type-2a fibers [38]. The single fiber analysis by catalytic histochemistry on serial sections of the TA muscle confirmed this distribution of nNOS: nNOS-specific diaphorase activity was enriched in type-2 oxidative fibers, Thus, the appearance of nNOS in skeletal muscles of mice resembles that of rats, in which nNOS is enriched in fast-twitch (type-2) oxidative fibers [2], while the enzyme is more evenly distributed throughout all fiber types (at least) in human vastus lateralis muscle [39; 40].

4.2 Mitochondrial density/activity in nNOS-KO mice and WT littermates

Highest CS activity levels were found in homogenates of GC-med muscle, while significantly lower CS activities were evidenced in RF and GC-lat muscles of both mouse strains. Strikingly, the differences in CS activities between the nNOS-KO mice and their WT littermates were likewise inconsistent within the muscles: pronounced differences in CS activities between the two mouse strains were found in TA and GC-

lat muscles, while only minor differences were present in RF muscle. We understand such differences in CS activities between the nNOS-KO mice and their WT littermates as quantitative indicators for a pool of mitochondria that depends on the manifestation of nNOS. It is striking that striated muscles with such a large nNOS-dependent mitochondrial pool, e.g. TA and GC-lat muscles, are those that consist to a greater extent of type-2 oxidative fiber types [38; 41; 42; 43].

The mitochondrial content of skeletal muscles in nNOS-KO mice and WT mice has previously been assessed several times. Morphometry after EM analysis performed by Schild and colleagues revealed a trend towards reduced mitochondria density in the GC muscle of nNOS-KO mice compared to WT mice, although they simultaneously observed non-significantly higher CS levels determined in immunoblots and significantly elevated CS activity [44]. Wadley and colleagues found significantly higher mRNA levels of mitochondria-associated marker genes (NRFs, mtTFA) in the EDL muscle (with a similar muscle fiber composition as TA) but not in the SOL muscles of nNOS-KO mice than in those of WT mice [13]. At the same time, CS activities in the EDL were not significantly higher in the nNOS-KO mice compared to the WT mice [13]. It has furthermore been reported that the mitochondrial DNA levels in TA muscles do not significantly differ between nNOS-KO and WT mice [14] although the graph presented in the paper shows a clear trend for lower mitochondrial DNA levels in the nNOS-KO strain. Taken together, the previous publications on this topic do not draw a consistent picture of the quantitative incidence of mitochondria in skeletal muscles of nNOS-KO mice compared to WT mice. It seems possible that specific bias of the indirect methods that were applied to determine the mitochondria content in these studies are (at least partially) responsible for the inconsistency of the results.

To overcome this methodological drawback, we performed morphometry after EM analysis, which is considered as the ‘gold standard’ method for the determination of the compartmental composition in tissues due to the direct visualization and quantification of the cellular structures [45]. In this investigation, we found the mitochondrial volume density in the oxidative proportion of the TA muscle to be significantly lower in nNOS-KO mice than in their WT littermates. In contrast, when we subjected the non-oxidative RF muscle to the same morphometric protocol, the values for mitochondrial volume density differed only non-significantly between the two mouse strains. These findings are in line to the conclusion drawn on the basis of

the CS activity assay that an nNOS-dependent mitochondrial pool exists in type-2 oxidative skeletal muscle fibers.

Remarkably, on the electron micrographs we have never observed myopathic structural changes of the mitochondrial phenotype in the skeletal muscles of the nNOS-KO mice, which had been previously reported [14; 28]. The reasons for these contradictory findings are unknown.

4.3 nNOS alpha-isoform is enriched in oxidative striated muscles of mice

Our immunoblotting investigation is the first one in which the relation between 160-kDa alpha- and 140-kDa beta-isoforms of nNOS was systematically quantified in murine striated muscles. Highest concentrations of the alpha-isoform of nNOS were seen in TA, while almost equal levels of alpha- and beta-isoforms were present in RF and PLNT muscles of mice. All other muscles exhibited an nNOS alpha-isoform/beta-isoform ratio between these two outsider values. As mentioned above, TA muscle is composed of a high proportion of fast-twitch oxidative 2d/x and 2a fibers, while RF and PLNT muscles consist almost entirely of type-2b glycolytic fibers [38]. We therefore suspect that the alpha-isoform of nNOS is enriched in type-2 oxidative fibers (type-2d/x and type-2a), while type-2b fibers contain equivalent levels of nNOS alpha- and beta-isoforms. This hypothesis has to be confirmed by other approaches, e.g. fiber typing in combination with anti-nNOS immunohistochemistry, which however is a difficult task because a specific antibody against the nNOS beta-isoform is not available.

When we performed regression analysis with the data sets from the CS activity assay and the quantitative nNOS-immunoblotting we found a significant positive relation between the differences in mitochondrial density of nNOS-KO mice and their WT littermates and the expression levels of the nNOS alpha-isoform. The statistical link between the nNOS alpha-isoform expression levels and the CS-dependent activity does however not allow concluding that this nNOS-variant is the enzyme that specifically controls the extent of the nNOS-dependent mitochondrial pool in murine skeletal muscles with a high proportion of oxidative fibers. In fact, additional investigations must be undertaken in order to demonstrate such a potential functional relationship between nNOS alpha-isoform and mitochondrial density.

Interestingly, it has recently been shown that the nNOS alpha-isoform but not the beta-isoform is translocated to the nucleus in C2C12 cells via an alpha1-syntrophin

binding leading to S-nitrosylation of the transcriptions factor CREB and subsequent mitochondriogenesis owing to the up-regulation of mitochondrial genes such as TFAM and MtCO1 [46]. This sequence of cellular events could be (at least be part of) the molecular cascade(s) that elicits the nNOS alpha-isoform-dependent higher mitochondrial density *in vivo*, as described here.

This investigation was performed on striated muscles of resting mice. It is possible that the statistical relations described here (e.g. between nNOS alpha-isoform and mitochondrial activity in type-2 fibers) are altered during/after endurance exercise when both nNOS levels/activities [46] and mitochondrial density are increased. Further research has to be done to clarify this issue.

4.4 Shift in favor of the nNOS alpha-isoform in PGC-1alpha transgenic mice

Emanating from the observation nNOS alpha-isoform is related to the mitochondrial density in murine skeletal muscle, we assessed whether the expression patterns of the nNOS variants are regulated in relation to genes that control the mitochondrial density. For this task, we focused to study the relation of nNOS to PGC-1alpha, which belongs to a family of established (co)factors that drive the quantity of mitochondria in many tissues, including skeletal muscle [30; 31]. This decision was based on the observation that even type-2 fibers express low levels of PGC-1alpha in WT mice [30], and, thus, exhibit the potential to adapt to the strong increase in PGC-1alpha expression induced by the genetic manipulation of the TG mice.

In detergent extracts of striated muscles with many type-2 oxidative fibers, we observed a significant shift in the expression patterns of the nNOS isoforms in favor of the alpha-isoform and at the expense of the beta-isoform in PGC-1alpha TG mice compared to their WT littermates. These findings suggest that PGC-1alpha has an up-stream impact on the regulation of the nNOS isoforms expression patterns by increasing the levels of the alpha-isoform in combination with the simultaneous down-regulation of the beta-isoform in these muscles. Interestingly, the nitrite production rates in VL muscle extracts of PGC-1alpha TG mice and WT mice were alike indicating that the nNOS alpha- and beta-isoforms exhibit similar catalytic NOS activities. This conclusion is in accordance to the findings obtained with the recombinant proteins [3].

As signaling enzyme, nNOS is involved in the regulation of many physiological processes in skeletal muscle fibers [15]. The nNOS/NO system lowers in an

autocrine fashion the contraction force [1], contributes to glucose uptake during contraction/exercise in a complex pattern [47; 48; 49], exhibits a positive allosteric effect on phosofructokinase-1 activity [50] and impacts the lipid metabolism [44] in skeletal muscle fibers. Furthermore, nNOS has likewise a positive influence on the capillary density, which is reduced in nNOS-KO mice [33]. Common consequence of this wide spectrum of functions is the increase in glucose availability in the skeletal fibers either by accelerating anaplerotic reactions or inhibition of carbohydrate oxidation.

PGC-1alpha has likewise a modulatory effect on a broad range of metabolic processes in skeletal muscles. Originally identified as a master co-regulating factor of mitochondriogenesis via interaction with multiple transcription factors, it was subsequently shown that PGC-1alpha also modulates numerous other metabolic processes, which prevent glucose consumption and promote lipid oxidation [34]. It is also established that PGC-1alpha increases capillary density and angiogenesis in skeletal muscle [51]. Thus, from a biological point-of-view it is conceivable that nNOS and PGC-1alpha may functionally converge in type-2 oxidative muscle fibers: cell signaling processes of both proteins merge e.g. into an increase of the intrafibrar glucose availability. Because the increases in mitochondrial density were only inconsistently associated with the altered nNOS-isoform expression patterns in striated muscles of PGC-1alpha TG mice we suggest that the two proteins are not obligatory linked to induce the biogenesis of new mitochondria.

The findings of this study imply that PGC-1alpha is located up-stream of nNOS within the signaling chain inside type-2 oxidative skeletal muscle fibers to induce the shift in nNOS expression in favor of the nNOS alpha-isoform. Other studies revealed that PGC-1alpha might also be situated down-stream of nNOS action: NO is capable to increase PGC-1alpha expression to up-regulate mitochondrial biogenesis in many cells and tissues [52], including L6 myotubes [53].

Baldelli and colleagues [54] have recently proposed that both nNOS and PGC-1alpha are integrative linkers within a molecular network that commonly influences the metabolism in muscle cells/fibers. Our *in vivo* findings specify this hypothesis demonstrating that a nNOS-dependent pool of mitochondria is established in type-2 oxidative skeletal muscle fibers related to the nNOS alpha-isoform, which may be considerably up-regulated by PGC-1alpha action. Therefore, the interaction between

nNOS and PGC-1alpha appears to be nNOS isoform-specific and seems to involve the mutual regulation of both proteins in a fiber type-specific manner.

5. Conclusions

Combination of the conclusions on our main findings (1. preponderance of nNOS in type-2 oxidative skeletal muscle fibers, 2. existence of a nNOS-dependent mitochondrial pool in type-2 oxidative skeletal muscle fibers, 3. correlation between nNOS-alpha isoform and this nNOS-dependent mitochondrial pool in type-2 oxidative fibers and 4. up-regulation of the nNOS-alpha isoform in striated muscles of PGC-1alpha TG mice) leads us to hypothesize that the two signaling systems functionally converge in type-2 oxidative skeletal muscle fibers of mice.

Acknowledgements

We would like to thank Bettina Cardel, Daniela Miescher, Laura Schaad, Franziska Graber and Adolfo Odriozola for their excellent technical support.

Grants

This work was supported by a grant of the Swiss National Science Foundation (SNF) to Oliver Baum (grant number 320030-144167).

Disclosures

No conflicts of interest are declared by the authors.

References

[1] L. Kobzik, M.B. Reid, D.S. Bredt, J.S. Stamler, Nitric oxide in skeletal muscle, Nature 372 (1994) 546-548.

[2] G. Planitzer, A. Miethke, O. Baum, Nitric oxide synthase-1 is enriched in fast-twitch oxidative myofibers, Cell Tissue Res. 306 (2001) 325-333.

[3] J.E. Brenman, D.S. Chao, S.H. Gee, A.W. McGee, S.E. Craven, D.R. Santillano, Z. Wu, F. Huang, H. Xia, M.F. Peters, S.C. Froehner, D.S. Bredt, Interaction of nitric oxide synthase with the postsynaptic density protein PSD-95 and alpha1-syntrophin mediated by PDZ domains, Cell 84 (1996) 757-767.

[4] A. Abdelmoity, R.C. Padre, K.E. Burzynski, J.T. Stull, K.S. Lau, Neuronal nitric oxide synthase localizes through multiple structural motifs to the sarcolemma in mouse myotubes, FEBS Lett. 482 (2000) 65-70.

[5] Y. Lai, J. Zhao, Y. Yue, D. Duan, alpha2 and alpha3 helices of dystrophin R16 and R17 frame a microdomain in the alpha1 helix of dystrophin R17 for neuronal NOS binding, Proc. Natl. Acad. Sci. U. S. A. 110 (2013) 525-530.

[6] S.Q. Harper, Molecular dissection of dystrophin identifies the docking site for nNOS, Proc. Natl. Acad. Sci. U. S. A. 110 (2013) 387-388.

[7] A.E. Molza, K. Mangat, E. Le Rumeur, J.F. Hubert, N. Menhart, O. Delalande, Structural basis of neuronal nitric-oxide synthase interaction with dystrophin repeats 16 and 17, J. Biol. Chem. 290 (2015) 29531-29541.

[8] J.G. Tidball, M. Wehling-Henricks, Nitric oxide synthase deficiency and the pathophysiology of muscular dystrophy, J. Physiol. 592 (2014) 4627-4638.

[9] D.L. Rebolledo, M.J. Kim, N.P. Whitehead, M.E. Adams, S.C. Froehner, Sarcolemmal targeting of nNOSmu improves contractile function of mdx muscle, Hum. Mol. Genet. 25 (2016) 158-166.

[10] D.G. Allen, N.P. Whitehead, S.C. Froehner, Absence of dystrophin disrupts skeletal muscle signaling: roles of Ca2+, reactive oxygen species, and nitric oxide in the development of muscular dystrophy, Physiol. Rev. 96 (2016) 253-305.

[11] Y. Moon, J.E. Balke, D. Madorma, M.P. Siegel, G. Knowels, P. Brouckaert, E.S. Buys, D.J. Marcinek, J.M. Percival, Nitric oxide regulates skeletal muscle fatigue, fiber type, microtubule organization, and mitochondrial ATP synthesis efficiency through cGMP-dependent mechanisms, Antioxid Redox Signal 26 (2017) 966-985.

[12] Y. Sha, H.E. Marshall, S-nitrosylation in the regulation of gene transcription, Biochim. Biophys. Acta 1820 (2012) 701-711.

[13] G.D. Wadley, J. Choate, G.K. McConell, NOS isoform-specific regulation of basal but not exercise-induced mitochondrial biogenesis in mouse skeletal muscle, J. Physiol. 585 (2007) 253-262.

[14] C. De Palma, F. Morisi, S. Pambianco, E. Assi, T. Touvier, S. Russo, C. Perrotta, V. Romanello, S. Carnio, V. Cappello, P. Pellegrino, C. Moscheni, M.T. Bassi, M. Sandri, D. Cervia, E. Clementi, Deficient nitric oxide signalling impairs skeletal muscle growth and performance: involvement of mitochondrial dysregulation, Skelet Muscle 4 (2014) 22.

[15] J.S. Stamler, G. Meissner, Physiology of nitric oxide in skeletal muscle, Physiol. Rev. 81 (2001) 209-237.

[16] T.J. Koh, J.G. Tidball, Nitric oxide synthase inhibitors reduce sarcomere addition in rat skeletal muscle, J. Physiol. 519 (1999) 189-196.

[17] N. Ito, U.T. Ruegg, A. Kudo, Y. Miyagoe-Suzuki, S. Takeda, Activation of calcium signaling through Trpv1 by nNOS and peroxynitrite as a key trigger of skeletal muscle hypertrophy, Nat. Med. 19 (2013) 101-106.

[18] G. Samengo, A. Avik, B. Fedor, D. Whittaker, K.H. Myung, M. Wehling-Henricks, J.G. Tidball, Age-related loss of nitric oxide synthase in skeletal muscle causes reductions in calpain S-nitrosylation that increase myofibril degradation and sarcopenia, Aging Cell 11 (2012) 1036-1045.

[19] G.D. Thomas, P.W. Shaul, I.S. Yuhanna, S.C. Froehner, M.E. Adams, Vasomodulation by skeletal muscle-derived nitric oxide requires alpha-syntrophin-mediated sarcolemmal localization of neuronal Nitric oxide synthase, Circ. Res. 92 (2003) 554-560.

[20] D.M. Hirai, S.W. Copp, S.K. Ferguson, C.T. Holdsworth, K.S. Hageman, D.C. Poole, T.I. Musch, Neuronal nitric oxide synthase regulation of skeletal muscle functional hyperemia: exercise training and moderate compensated heart failure, Nitric Oxide 74 (2018) 1-9.

[21] Y.M. Kobayashi, E.P. Rader, R.W. Crawford, N.K. Iyengar, D.R. Thedens, J.A. Faulkner, S.V. Parikh, R.M. Weiss, J.S. Chamberlain, S.A. Moore, K.P. Campbell, Sarcolemma-localized nNOS is required to maintain activity after mild exercise, Nature 456 (2008) 511-515.

[22] L. Da Silva-Azevedo, S. Jahne, C. Hoffmann, D. Stalder, M. Heller, A.R. Pries, A. Zakrzewicz, O. Baum, Up-regulation of the peroxiredoxin-6 related metabolism of reactive oxygen species in skeletal muscle of mice lacking neuronal nitric oxide synthase, J. Physiol. 587 (2009) 655-668.

[23] G.K. Sakellariou, D. Pye, A. Vasilaki, L. Zibrik, J. Palomero, T. Kabayo, F. McArdle, H. Van Remmen, A. Richardson, J.G. Tidball, A. McArdle, M.J. Jackson, Role of superoxide-nitric oxide interactions in the accelerated age-related loss of muscle mass in mice lacking Cu,Zn superoxide dismutase, Aging Cell 10 (2011) 749-760.

[24] M.J. Jackson, Redox regulation of muscle adaptations to contractile activity and aging, J Appl Physiol (1985) 119 (2015) 163-171.

[25] S.K. Powers, E.E. Talbert, P.J. Adhihetty, Reactive oxygen and nitrogen species as intracellular signals in skeletal muscle, J. Physiol. 589 (2011) 2129-2138.

[26] Y. Wang, D.C. Newton, G.B. Robb, C.L. Kau, T.L. Miller, A.H. Cheung, A.V. Hall, S. VanDamme, J.N. Wilcox, P.A. Marsden, RNA diversity has profound effects on the translation of neuronal nitric oxide synthase, Proc. Natl. Acad. Sci. U. S. A. 96 (1999) 12150-12155.

[27] F. Silvagno, H. Xia, D.S. Bredt, Neuronal nitric-oxide synthase-mu, an alternatively spliced isoform expressed in differentiated skeletal muscle, J. Biol. Chem. 271 (1996) 11204-11208.

[28] J.M. Percival, K.N. Anderson, P. Huang, M.E. Adams, S.C. Froehner, Golgi and sarcolemmal neuronal NOS differentially regulate contraction-induced fatigue and vasoconstriction in exercising mouse skeletal muscle, J. Clin. Invest. 120 (2010) 816-826.

[29] O. Baum, S. Schlappi, F.A. Huber-Abel, A. Weichert, H. Hoppeler, A. Zakrzewicz, The beta-isoform of neuronal nitric oxide synthase (nNOS) lacking the PDZ domain is localized at the sarcolemma, FEBS Lett. 585 (2011) 3219-3223.

[30] J. Lin, H. Wu, P.T. Tarr, C.Y. Zhang, Z. Wu, O. Boss, L.F. Michael, P. Puigserver, E. Isotani, E.N. Olson, B.B. Lowell, R. Bassel-Duby, B.M. Spiegelman, Transcriptional co-activator PGC-1 alpha drives the formation of slow-twitch muscle fibres, Nature 418 (2002) 797-801.

[31] C. Handschin, B.M. Spiegelman, Peroxisome proliferator-activated receptor gamma coactivator 1 coactivators, energy homeostasis, and metabolism, Endocr. Rev. 27 (2006) 728-735.

[32] P.L. Huang, T.M. Dawson, D.S. Bredt, S.H. Snyder, M.C. Fishman, Targeted disruption of the neuronal nitric oxide synthase gene, Cell 75 (1993) 1273-1286.

[33] O. Baum, M. Vieregge, P. Koch, S. Gul, S. Hahn, F.A. Huber-Abel, A.R. Pries, H. Hoppeler, Phenotype of capillaries in skeletal muscle of nNOS-knockout mice, Am. J. Physiol. Regul. Integr. Comp. Physiol. 304 (2013) R1175-1182.

[34] S. Summermatter, O. Baum, G. Santos, H. Hoppeler, C. Handschin, Peroxisome proliferator-activated receptor {gamma} coactivator 1{alpha} (PGC-1{alpha}) promotes skeletal muscle lipid refueling in vivo by activating de novo lipogenesis and the pentose phosphate pathway, J. Biol. Chem. 285 (2010) 32793-32800.

[35] O. Baum, A. Miethke, A. Wockel, G. Willerding, G. Planitzer, The specificity of the histochemical NADPH diaphorase reaction for nitric oxide synthase-1 in skeletal muscles is increased in the presence of urea, Acta Histochem. 104 (2002) 3-14.

[36] O. Baum, E. Torchetti, C. Malik, B. Hoier, M. Walker, P.J. Walker, A. Odriozola, F. Graber, S.A. Tschanz, J. Bangsbo, H. Hoppeler, C.D. Askew, Y. Hellsten, Capillary ultrastructure and mitochondrial volume density in skeletal muscle in relation to reduced exercise capacity of patients with intermittent claudication, Am. J. Physiol. Regul. Integr. Comp. Physiol. 310 (2016) R943-951.

[37] P. Meier, M. Renga, H. Hoppeler, O. Baum, The impact of antioxidant supplements and endurance exercise on genes of the carbohydrate and lipid metabolism in skeletal muscle of mice, Cell Biochem. Funct. 31 (2013) 51-59.

[38] D. Bloemberg, J. Quadrilatero, Rapid determination of myosin heavy chain expression in rat, mouse, and human skeletal muscle using multicolor immunofluorescence analysis, PLoS One 7 (2012) e35273.

[39] R. Gossrau, Caveolin-3 and nitric oxide synthase I in healthy and diseased skeletal muscle, Acta Histochem. 100 (1998) 99-112.

[40] U. Frandsen, L. Hoffner, A. Betak, B. Saltin, J. Bangsbo, Y. Hellsten, Endurance training does not alter the level of neuronal nitric oxide synthase in human skeletal muscle, J. Appl. Physiol. 89 (2000) 1033-1038.

[41] L. Gorza, Identification of a novel type 2 fiber population in mammalian skeletal muscle by combined use of histochemical myosin ATPase and anti-myosin monoclonal antibodies, J. Histochem. Cytochem. 38 (1990) 257-265.

[42] O. Agbulut, P. Noirez, F. Beaumont, G. Butler-Browne, Myosin heavy chain isoforms in postnatal muscle development of mice, Biology of the Cell 95 (2003) 399-406.

[43] V. Augusto, C.R. Padovani, G.E.R. Campos, Skeletal muscle fiber types in C57BL6J mice, Braz J Morphol Sci 21 (2004) 89-94.

[44] L. Schild, I. Jaroscakova, U. Lendeckel, G. Wolf, G. Keilhoff, Neuronal nitric oxide synthase controls enzyme activity pattern of mitochondria and lipid metabolism, FASEB J. 20 (2006) 145-147.

[45] D.M. Medeiros, Assessing mitochondria biogenesis, Methods 46 (2008) 288-294.

[46] K. Aquilano, S. Baldelli, M.R. Ciriolo, Nuclear recruitment of neuronal nitric-oxide synthase by alpha-syntrophin is crucial for the induction of mitochondrial biogenesis, J. Biol. Chem. 289 (2014) 365-378.

[47] G.K. McConell, S. Rattigan, R.S. Lee-Young, G.D. Wadley, T.L. Merry, Skeletal muscle nitric oxide signaling and exercise: a focus on glucose metabolism, Am. J. Physiol. Endocrinol. Metab. 303 (2012) E301-307.

[48] Y.H. Hong, A.C. Betik, D. Premilovac, R.M. Dwyer, M.A. Keske, S. Rattigan, G.K. McConell, No effect of NOS inhibition on skeletal muscle glucose uptake during in situ hindlimb contraction in healthy and diabetic Sprague-Dawley rats, Am. J. Physiol. Regul. Integr. Comp. Physiol. 308 (2015) R862-871.

[49] Y.H. Hong, C. Yang, A.C. Betik, R.S. Lee-Young, G.K. McConell, Skeletal muscle glucose uptake during treadmill exercise in neuronal nitric oxide synthase-mu knockout mice, Am. J. Physiol. Endocrinol. Metab. 310 (2016) E838-845.

[50] M. Wehling-Henricks, M. Oltmann, C. Rinaldi, K.H. Myung, J.G. Tidball, Loss of positive allosteric interactions between neuronal nitric oxide synthase and phosphofructokinase contributes to defects in glycolysis and increased fatigability in muscular dystrophy, Hum. Mol. Genet. 18 (2009) 3439-3451.

[51] J. Chinsomboon, J. Ruas, R.K. Gupta, R. Thom, J. Shoag, G.C. Rowe, N. Sawada, S. Raghuram, Z. Arany, The transcriptional coactivator PGC-1alpha

mediates exercise-induced angiogenesis in skeletal muscle, Proc. Natl. Acad. Sci. U. S. A. 106 (2009) 21401-21406.

[52] E. Nisoli, E. Clementi, C. Paolucci, V. Cozzi, C. Tonello, C. Sciorati, R. Bracale, A. Valerio, M. Francolini, S. Moncada, M.O. Carruba, Mitochondrial biogenesis in mammals: the role of endogenous nitric oxide, Science 299 (2003) 896-899.

[53] V.A. Lira, D.L. Brown, A.K. Lira, A.N. Kavazis, Q.A. Soltow, E.H. Zeanah, D.S. Criswell, Nitric oxide and AMPK cooperatively regulate PGC-1 in skeletal muscle cells, J. Physiol. 588 (2010) 3551-3566.

[54] S. Baldelli, D. Lettieri Barbato, G. Tatulli, K. Aquilano, M.R. Ciriolo, The role of nNOS and PGC-1alpha in skeletal muscle cells, J. Cell Sci. 127 (2014) 4813-4820.

Figure legends

Fig 1: Catalytic histochemistry to determine the statistical relationship between nNOS-specific diaphorase and succinate dehydrogenase activities at the muscle fiber level. A,B: Representative serial sections of the TA muscle subjected to catalytic histochemistry to monitor the activity of nNOS-specific diaphorase (A) and mitochondria-related succinate dehydrogenase (SDH; B). Note that the larger skeletal muscle fibers (asterisks) contain simultaneously less nNOS-diaphorase and SDH activities than smaller ones. **C:** Negative control for nNOS-specific diaphorase reaction shown in A. **D:** Linear regression analysis revealing a significant positive relation between nNOS-specific diaphorase and SDH activities. The plot mirrors the densitometric values in skeletal muscle fibers from the oxidative portion of TA muscle. Shown is the Pearson product-moment correlation coefficient (r) together with its probability (*P*). Bear in mind that the TA muscle of mice is almost exclusively composed of type-2 skeletal muscle fibers.

Fig 2: Morphometry after transmission electron microscopy to estimate mitochondria volume density in tibialis anterior (TA) and rectus femoris (RF) muscles of nNOS-KO mice and their WT littermates. A: Representative electron micrographs of TA muscle from an nNOS-KO mouse and a WT littermate each depicting a cross-sectioned capillary profile surrounded by profiles of three skeletal muscle fibers. Note the subsarcolemmal and the myofibrillar pool of mitochondria manifested in all muscle fibers. **B, C:** Morphometric quantification of the total mitochondrial volume density in skeletal muscle fibers as well as its allocation among the subsarcolemmal and intrafibrillar pools in TA muscle (B) and RF muscle (C) of nNOS-KO mice and WT littermates. Mean values ± SD, *n*=5 for both mouse strains. Significance level: *: $P \leq 0.05$.

Fig 3: Inconsistent expression of nNOS in striated muscles of C57/Bl6 mice. A: 50 µg of protein from detergent solubilsates of eight striated muscles taken from C57BL/6-mice were subjected to immunoblot analysis with a polyclonal anti-nNOS antibody (anti-C-terminus). **B:** The blot matrices were stained with Ponceau Red after immunoblotting for loading control. **C:** The nNOS-immunoreactive bands in the muscle solubilsates were densitometrically quantified and normalized to protein

loading assessed by Ponceau S-staining in order to depict the nNOS level in each muscle. The concentration of nNOS bands in TA muscle was set as 100%. Mean values ± SD, *n*=4. **D:** The expression ratio between the 160-kDa (alpha)- and 140-kDa (beta)-isoforms of nNOS in striated muscles of mice, as determined by densitometry of the nNOS-bands after immunoblotting. Mean values ± SD, *n*=4.

Fig 4: Citrate synthase assay to establish the statistical relationship between alpha-isoform expression and mitochondrial density in striated muscle. A: Citrate synthase (CS) activity was assessed in homogenates of eight striated muscles from nNOS-KO mice and their WT littermates. Mean values ± SD, *n*=3 triplicates for both strains. *: $P \leq 0.05$. **B:** Linear regression analysis revealing the difference in CS activity between WT mice and nNOS-KO mice (data from Fig 4A) to be significantly positive related to the relative nNOS alpha-isoform levels in striated muscles of WT mice (data from Fig 1C and 1D). Shown is the Pearson product-moment correlation coefficient (r) together with its probability (*P*).

Fig 5: Shift of the nNOS-isoform expression patterns in striated muscles of PGC-1alpha-transgenic (TG) mice in comparison to WT mice. A: The nitrite production rates, which correspond to NOS activity, were assessed in RF muscle homogenates of PGC-1alpha-TG mice and their WT littermates by a fluorometric assay based on the nitrosylation of 2,3-diaminonaphthalene (DAN) to yield fluorescent 2,3-naphthotriazole. Mean values ± SD, *n*=6 duplicates for both strains. **B:** 50 µg of protein from solubilsates of RF muscle from PGC-1alpha-TG mice and WT mice were subjected to immunoblot analysis with a polyclonal anti-nNOS antibody. Note the increased levels of the nNOS alpha-isoform (160-kDa) relative to those of the beta-isoform (140-kDa) in the PGC-1alpha-TG mice compared to WT mice. **D:** Relation of the nNOS alpha- and beta-isoforms in detergent extracts of eight striated muscles from PGC-1alpha-tg mice and WT mice. The total nNOS concentration in each muscle was set as 100%. Mean values ± SD, *n*=6 for each group (with exceptions, see Supplementary Fig. 2). **E:** Densitometric quantification of total nNOS-immunoreactivity in detergent extracts of eight striated muscles from PGC-1alpha-tg mice and WT mice. The mean nNOS concentration in the WT mice was set as 100%. Mean values ± SD, *n*=6 for each group (with exceptions, see Supplementary Fig. 3).

Fig. 6: The shift in nNOS-isoform expression patterns is inconsistently related to the increase in mitochondria protein levels in muscle extracts of PGC-1alpha TG mice compared to WT littermates. Detergent extracts of the tongue **(A)**, the rectus femoris (RF) muscle **(B)** and six other striated muscles (Supplementary Fig 4) were subjected to immunoblotting with the mitochondria-specific OXPHOS antibody cocktail accounting for ATP5A of complex (C) 5 (55 kDa), SDHB of C2 (30 kDa) and NDUFB8 of C1 (20 kDa). * denote samples which contained higher ($P<0.05$) protein levels in the detergent extracts of the PGC-1alpha-TG mice than the WT mice. **C:** The changes in expression levels of mitochondrial ATP5A, quantified as representative example by densitometry of the immunoblot bands, were related to the shift in the expression of the nNOS-isoforms in the eight striated muscles of the PGC-1alpha-TG mice versus those of the WT mice.

Supporting information

Supplementary Fig. 1: Genotyping to demonstrate the absence of nNOS in the genome of nNOS-KO mice and its presence in that of their WT littermates. Using primers for exon-2 of the nNOS gene, a cDNA fragment of the neomycin resistance gene (280 base pairs (Bp) long) was amplified, whereas the presence of the nNOS gene was demonstrated by the amplification of its exon-2 containing fragment (117 Bp long).

Supplementary Figure 2: Shift of the nNOS isoform expression pattern in the rectus femoris muscle of PGC-1alpha transgenic (TG) mice in comparison to wild-type (WT) littermates (left side) and the Ponceau Red-stained blot matrices (right side). Note the higher expression of the alpha-isoform of nNOS (160 kDa) than the beta-isoform (140 kDa) in the PGC-1alpha TG mice than the WT mice. Shown are all immunoblots used for the densitometric analysis presented in Fig. 5C and 5D. Therefore, the densitometric values for nNOS-immunoreactive bands were normalized to the densitometric values of total protein loaded on the gels, as visualized by Ponceau Red-staining.

Supplementary Fig. 3: Immunoblot analysis for the quantification of nNOS isoform expression in eight striated muscles from PGC-1alpha-TG mice and their WT littermates. The immunoblots were used for the densitometric quantification of nNOS isoform expression shown in Fig. 5d and 5e. For both strains, detergent extracts of six mice (1-6) were subjected to the analysis. * denote samples which were not included into the densitometry due to inaccurate gel loading and/or incorrect supply with ECL reagent during development of immunoblots.

Supplementary Figure 4: Immunoblot analysis for the quantification of mitochondrial protein expression in six striated muscles from PGC-1alpha-TG mice and their WT littermates. For both strains, detergent extracts of six mice (1-6) were subjected to the analysis using the OXPHOS antibody cocktail accounting for ATP5A of complex (C) 5 (55 kDa), SDHB of C2 (30 kDa) and NDUFB8 of C1 (20 kDa) * denote samples which contained higher ($P<0.05$) protein levels in the detergent extracts of the PGC-1alpha-TG mice than the WT mice. Please note that

the immunoblots with the extracts of two additional striated muscles (RF and tongue) are presented in Fig. 6.

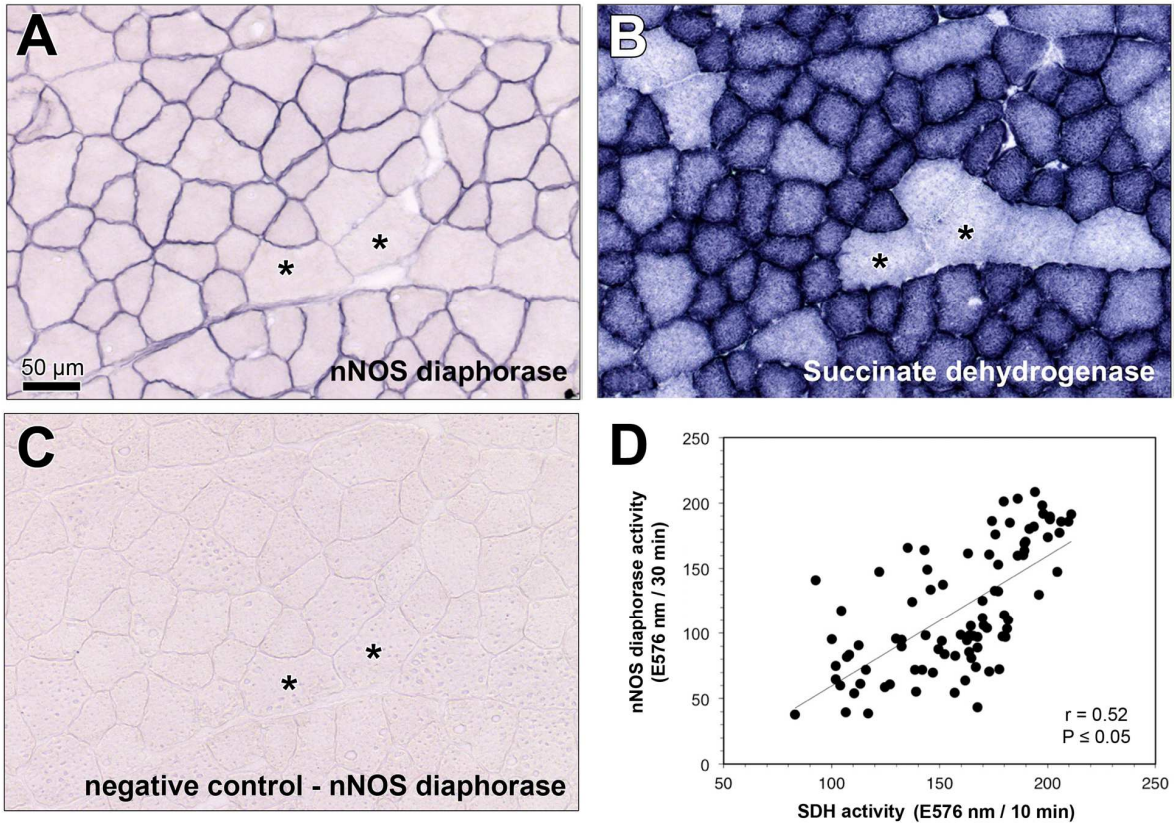

Baum et al.
Fig. 1

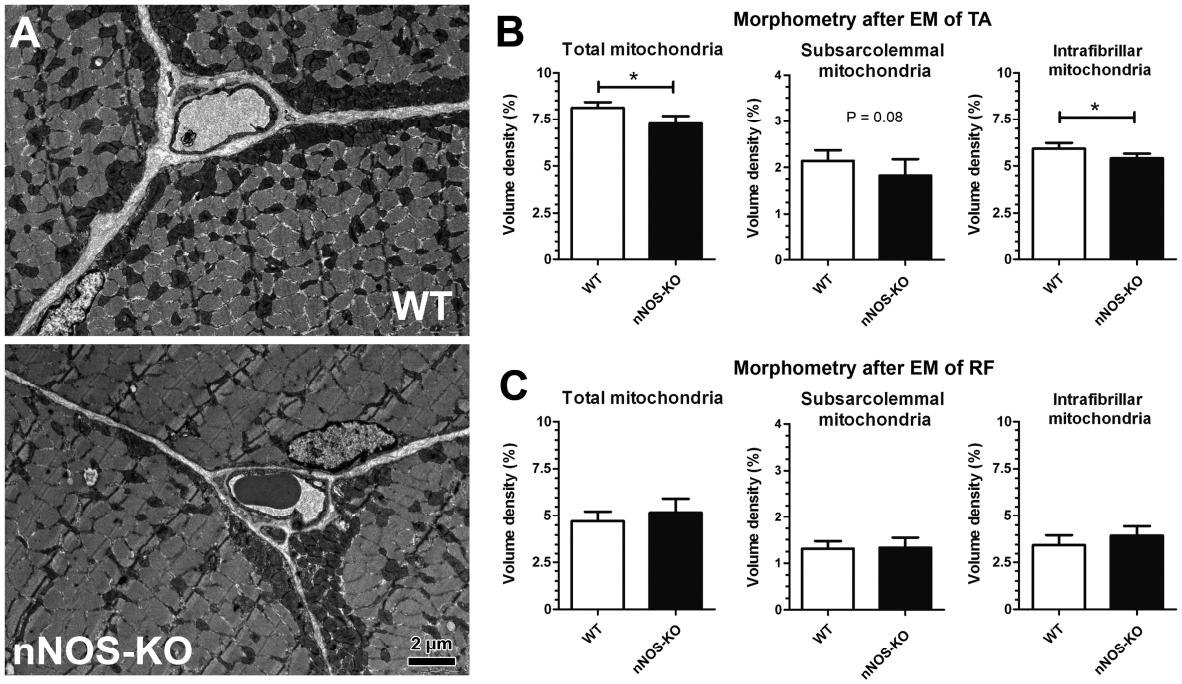

Baum et al.
Fig. 2

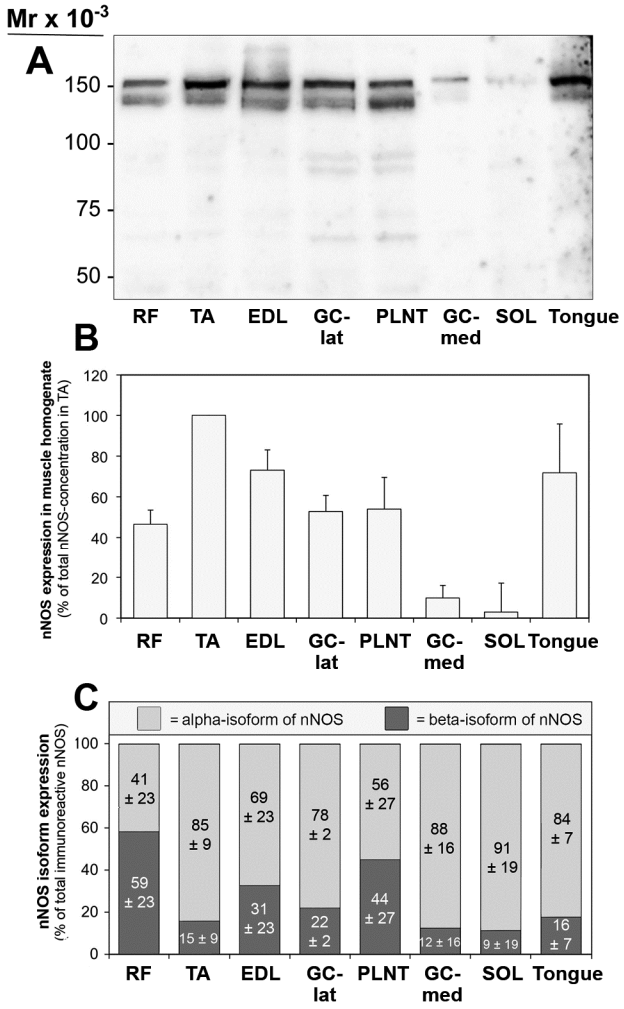

Baum et al.
Fig. 3

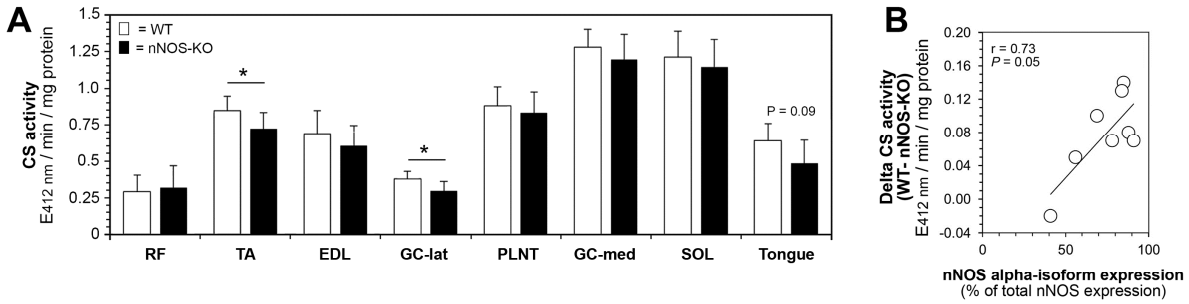

Baum et al.
Fig. 4

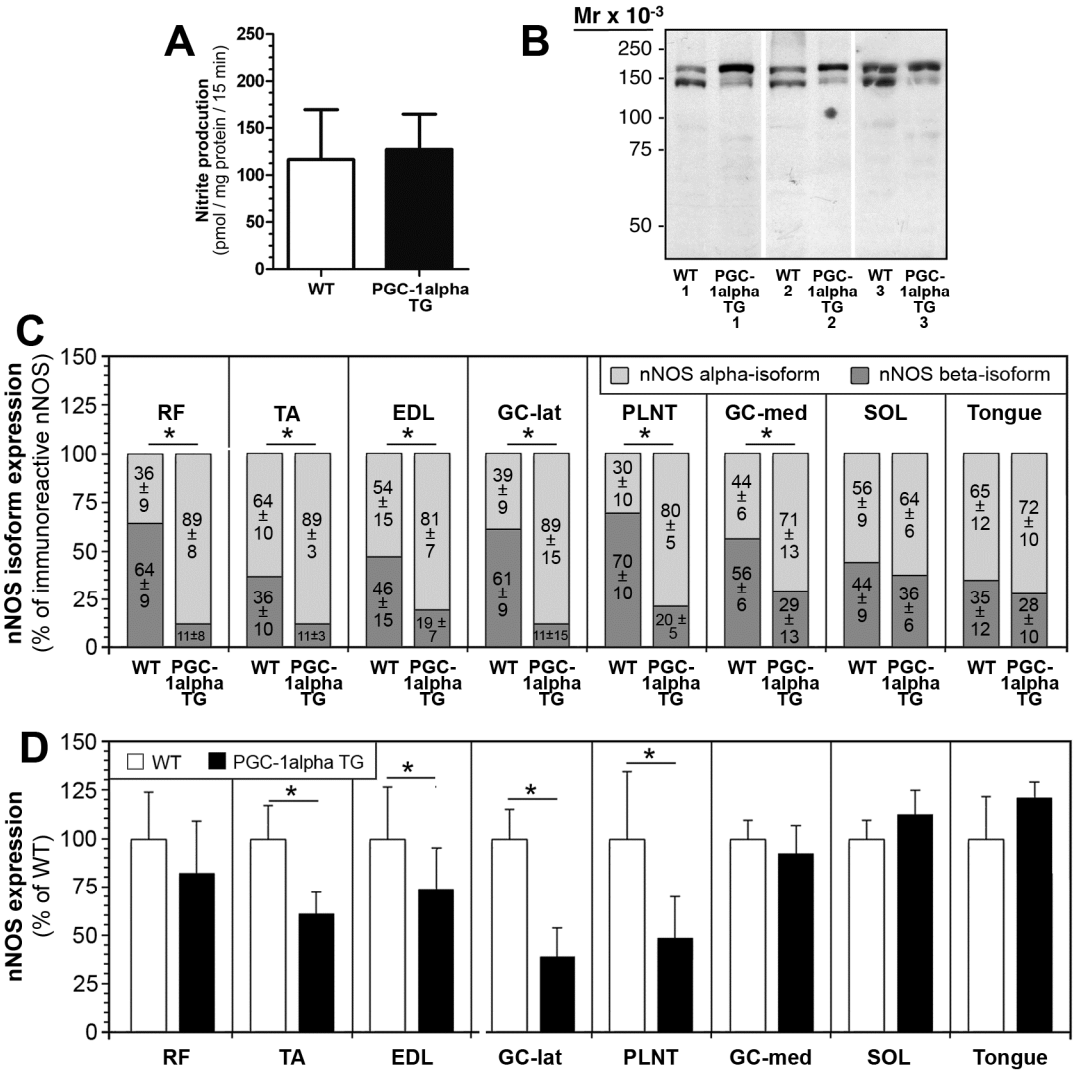

Baum et al.
Fig. 5

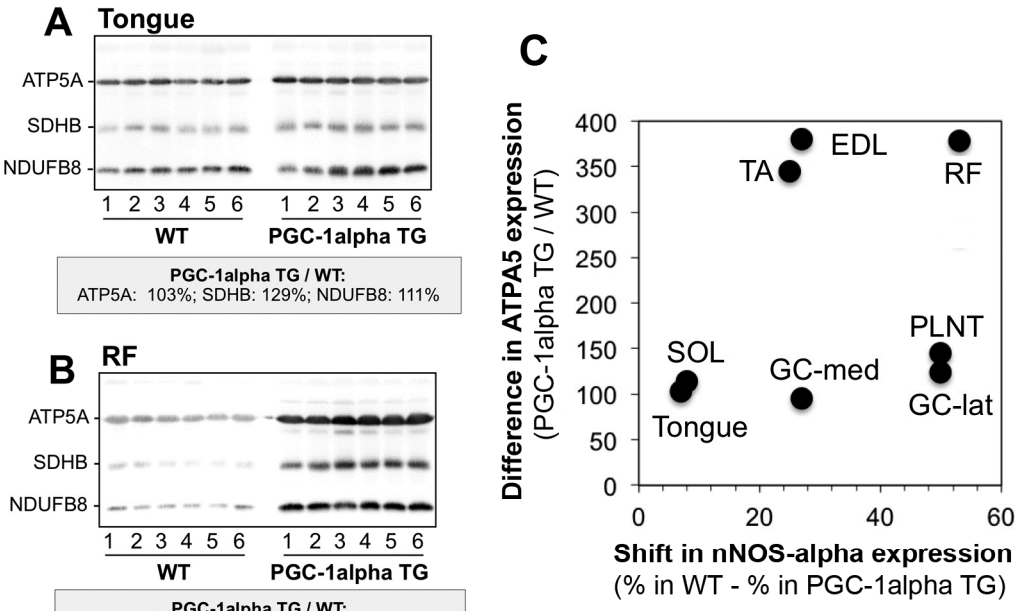

Baum et al.
Fig. 6

Highlights

- Highest nNOS-levels are expressed in type-2 oxidative fibers in striated muscles of mice
- Muscle nNOS-alpha isoform is positively related to differences in citrate synthase-activity between nNOS-KO-mice and WT-littermates
- nNOS alpha-isoform preponderates in striated muscles with many type-2 oxidative fibers
- In muscles of PGC-1alpha transgenic mice, nNOS-expression is shifted in favor of the alpha-isoform without consistent relationship to changes in the expression of mitochondrial markers